Paleobiology, page 1 of 17
DOI: 10.1017/pab.2017.32

PALEOBIOLOGY
A PUBLICATION OF THE Paleontological SOCIETY

Morphological evolution of the bivalve *Ptychomya* through the Lower Cretaceous of Argentina

Pablo S. Milla Carmona, Darío G. Lazo, and Ignacio M. Soto

Abstract.—The complex morphological evolution of the bivalve *Ptychomya* throughout the well-studied Agrio Formation in the Neuquén Basin (west-central Argentina, lower/upper Valanginian–lowest Barremian) constitutes an ideal opportunity to study evolutionary patterns and processes occurring at geological timescales. *Ptychomya* is represented in this unit by four species, the morphological variation of which needs to be temporally assessed to obtain a thorough picture of the evolution of the group. Here we use geometric morphometrics to measure variation in shell outline, ribbing pattern, and shell size in these species. We bracket the ages of our samples using a combination of ammonoid biostratigraphy and absolute ages and study the anagenetic pattern of evolution of each trait by means of paleontological time-series analysis and change tracking. We find that evolution in *Ptychomya* is mostly speciational, as the majority of traits show stasis, with the exceptions of shell size in *P. coihuicoensis* and shell outline in *P. windhauseni*, which seem to evolve directionally toward larger and higher shells, respectively. *Ptychomya* displays changes in its average morphology and disparity, which are the result of a mixture of taxonomic turnover and mosaic evolution of traits. Pulses of speciation would have been triggered by ecological opportunity, as they occur during the recovery of shallow-burrowing bivalve faunas after dysoxic events affecting the basin. On the other hand, the presence of directional patterns of evolution in *P. coihuicoensis* and *P. windhauseni* seems to be the result of a general shallowing-upward trend observed in the basin during the upper Hauterivian–lowest Barremian, as opposed to the cyclical paleoenvironmental stability inferred for the early/late Valanginian–early Hauterivian, which would have prompted stasis in *P. koeneni* and *P. esbelta*.

Pablo S. Milla Carmona and Darío G. Lazo. Universidad de Buenos Aires, Facultad de Ciencias Exactas y Naturales, Departamento de Ciencias Geológicas, Instituto de Estudios Andinos "Don Pablo Groeber" (IDEAN, UBA-CONICET), Pabellón II, Ciudad Universitaria, Buenos Aires C1428EGA, Argentina. E-mail: millacarmona@gl.fcen.uba.ar. dlazo@gl.fcen.uba.ar

Ignacio M. Soto. Universidad de Buenos Aires, Facultad de Ciencias Exactas y Naturales, Departamento de Ecología, Genética y Evolución, Instituto de Ecología, Genética y Evolución de Buenos Aires (IEGEBA, UBA- CONICET), Pabellón II, Ciudad Universitaria, Buenos Aires C1428EGA, Argentina. E-mail: soto@ege.fcen.uba.ar.

Accepted: 30 September 2017
Data available from the Dryad Digital Repository: http://doi.org/10.5061/dryad.gn5j6

Introduction

We have witnessed a resurgence of macroevolutionary studies over the past two decades. The development of pioneering methods exploiting genealogical data (e.g., Bokma 2002; Blomberg et al. 2003; Butler and King 2004; Hunt 2006; O'Meara et al. 2006; Hannisdal 2007; Adams and Collyer 2009) has allowed researchers to narrow the gap between the theoretical discussion that took place at the end of the last century (reviewed in Gould 2002) and the empirical evidence needed to support the different stances in the debate, especially regarding the relative frequency of different macroevolutionary patterns and the processes involved (Pagel et al. 2006; Hunt 2007; Harmon et al. 2010; Hopkins and Lidgard 2012). Methods taking advantage of phylogenetic data to infer patterns and processes shaping the evolution of clades have been of special importance in this regard (e.g., Harmon et al. 2003; Revell et al. 2007; Sidlauskas 2008). This in turn results from the wealth of recently generated data coming from living organisms and its potential integration with occurrences from the fossil record.

Despite comparable methodological advances, much less work is being carried out using the more traditional approach of tracking changes in morphology displayed by paleontological ancestor–descendant sequences through stratigraphic horizons. This procedure demands certain conditions that are only seldom met by fossil sequences, such as a sufficiently fine

 0094-8373/17

stratigraphic resolution coupled with a reliable geochronologic framework, adequate sample size, carefully measured morphology, and low taphonomic bias (Hunt 2008; Hannisdal 2007). Moreover, if the processes behind the patterns are to be addressed, a thorough knowledge of the biotic (e.g., ecological, ontogenetic) and abiotic (e.g., sedimentary, environmental) factors accompanying the evolution of the lineages of interest is needed, knowledge beyond the scope of many study cases and not always available. However, the strengths of this approach are evidenced by the few well-worked examples in which the ideal conditions are met (e.g., Cheetham 1986; Kucera and Malmgren 1998; Hunt et al. 2008; Payne et al. 2012). Importantly, it offers the opportunity to analyze directly (rather than infer) the anagenetic patterns of change shown by the studied lineages and to assess and discuss possible causes in an appropriate temporal and historical context. Overall, this remains the most direct way to study the evolutionary dynamics displayed by organisms over the course of millions of years, providing important insights into how organisms evolve in higher natural (e.g., temporal, geographical, taxonomic) scales.

The Neuquén Basin, located in the west-central region of Argentina, possesses one of the best Lower Cretaceous marine records of the Southern Hemisphere in terms of fossil abundance and stratigraphic completeness (Howell et al. 2005; Aguirre-Urreta et al. 2008). During that interval the region formed a back-arc basin flanked on its western margin by a volcanic island arc and flooded by the Pacific Ocean, forming a large, triangular marine embayment (Aguirre-Urreta et al. 2008; Lazo et al. 2008). Its depositional environment has been reconstructed as an open-marine, low-gradient ramp covered by a shallow sea, subject to moderate to strong fluctuations of relative sea level controlled by a combination of eustasy and local tectonics (Legarreta and Gulisano 1989; Lazo et al. 2008; Guler et al. 2013). The Agrio Formation, of lower/upper Valanginian to lowest Barremian age, can be divided into three subordinate units. The Pilmatué (lower/upper Valanginian–lower Hauterivian) and Agua de la Mula (upper Hauterivian–lowest Barremian) Members are represented by highly cyclic and fossiliferous shallow-marine deposits and are separated by the continental sandstones representing the Avilé Member, deposited during a short episode of marked sea-level fall in which most of the basin was emergent. The Agrio Formation has been the focus of exhaustive paleontological, sedimentological, and stratigraphic research (e.g., Legarreta and Gulisano 1989; Spalletti et al. 2001; Lazo 2006, 2007a; Aguirre-Urreta et al. 2008, 2011; Archuby et al. 2011; Pazos et al. 2012; Guler et al. 2013), something that has allowed the reconstruction of its paleoenvironmental and paleoecological history, as well as the development of high-resolution ammonoid-based biostratigraphic schemes and their correlations to the Tethys region (Aguirre-Urreta et al. 2007; Aguirre-Urreta and Rawson 2012).

The highly fossiliferous marine deposits of the Agrio Formation contain a rich fauna of benthic invertebrates in which bivalves are especially abundant. Prominent among them is the genus *Ptychomya* Agassiz (Veneroida: Astartidae), an extinct taxon of shallow-burrowing bivalves with a lower Valanginian to lowest Barremian local range (Milla Carmona et al. 2017). *Ptychomya* possesses a medium-sized (up to 8–10 cm in length, approximately), anteroposteriorly elongated shell, the anterior portion of which is short and rounded, whereas the posterior portion is about four times longer and exhibits a row of crenulations at each side of the opisthodetic ligament. The divaricate ornamentation is strikingly complex, with three series of ribs (one subcommarginal anterior and two subradial posterior) converging to form a series of compound ribs. The convergence of ribs defines, in turn, two series of chevrons. The first is defined by the convergence of the commarginal anterior and the long, subradial ventral posterior ribs, marking the limit between the anterior and posterior portions of the shell. The second is formed by the convergence of the long, subradial posterior ventral ribs with the subradial, shorter and slightly lower angled posterior dorsal ribs, running from the umbo toward the posterior ventral margin of the shell (Fig. 1). This eye-catching external morphology shows a comparably complex pattern of variation throughout the

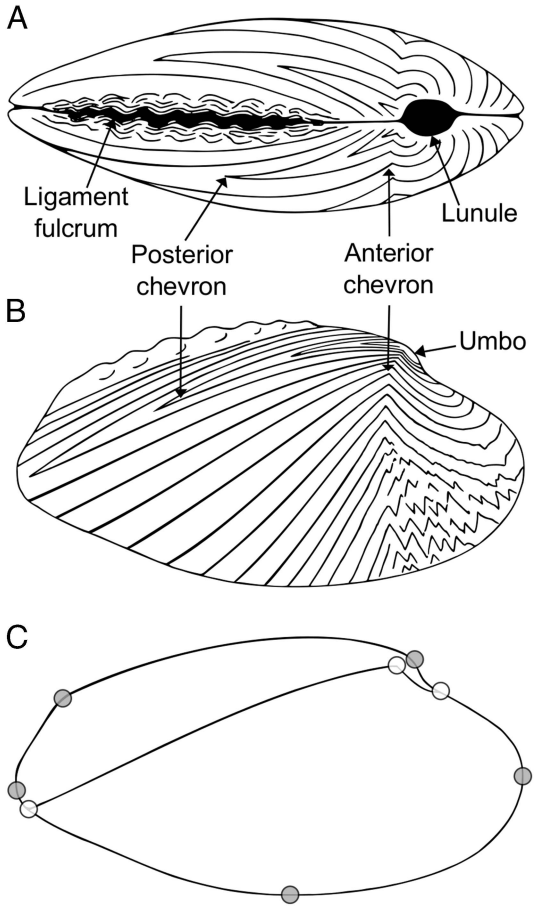

FIGURE 1. Schematic representation of *Ptychomya*, showing (A) dorsal and (B) left lateral views, as well as (C) the traits measured through geometric morphometrics. White circles indicate the position of the landmarks used for superimposition of the open curves measuring the shape of the reference pair of ribs (ribbing pattern), whereas gray circles indicate the position of the landmarks used for reconstruction and measurement of the full size of the shell. Modified from Milla Carmona et al. (2017).

Agrio Formation. However, although informally observed and acknowledged by researchers for over a century, the patterns of morphological change in *Ptychomya* have not been comprehensively assessed or even described.

Recently, much of the morphological variation was inferred to be of an interspecific nature, and the formerly monotypic genus was divided into four species: *P. koeneni* (lower Valanginian–upper Hauterivian, Fig. 2A), *P. esbelta* (upper Valanginian–lower Hauterivian, Fig. 2B), *P. coihuicoensis* (upper Hauterivian–lowest Barremian, Fig. 2C), and *P. windhauseni* (upper Hauterivian–lowest Barremian, Fig. 2D) (Milla Carmona et al. 2016, 2017). Although phylogenetic relationships among these four species have not been addressed yet, their well-framed stratigraphic occurrences suggest that *P. koeneni* constitutes the ancestral species from which the rest diverged at different times during the local history of the genus. The four species are abundant at various stratigraphic levels throughout the Agrio Formation, sometimes co-occurring. These properties, together with the well-studied depositional history of the Agrio Formation, configure an excellent opportunity for the study of macroevolutionary dynamics in deep time. Despite these advances, a question remains unanswered: How did *Ptychomya* evolve in the geographic and stratigraphic setting of the Neuquén Basin, and what were the evolutionary drivers involved?

We study here the anagenetic patterns of evolution displayed by the four species of *Ptychomya* mentioned earlier through the stratigraphic levels of the Agrio Formation using paleontological time-series analysis and change tracking. As recent compilations have shown, the different phenotypic aspects of lineages tend to evolve decoupled from each other (i.e., mosaic evolution). Thus, the analysis of single traits does not guarantee comprehensive reconstruction of the history of morphological change of a lineage (Hopkins and Lidgard 2012; Hunt et al. 2015), something that may be especially true for the case of the complex pattern of evolution exhibited by *Ptychomya*. To address this issue, we measure shell size as well as two conspicuous shape traits from the external morphology of the valves (shell outline and ribbing pattern) using geometric morphometrics. We then discuss (1) how patterns shown by the individual species lineages in different aspects of their morphology interact to give shape to the local evolution and diversification of the genus, (2) which biotic and/or abiotic factors could have driven the evolution of this group in the studied geographic and stratigraphic setting, and (3) how these findings fit into our present knowledge of macroevolutionary phenomena.

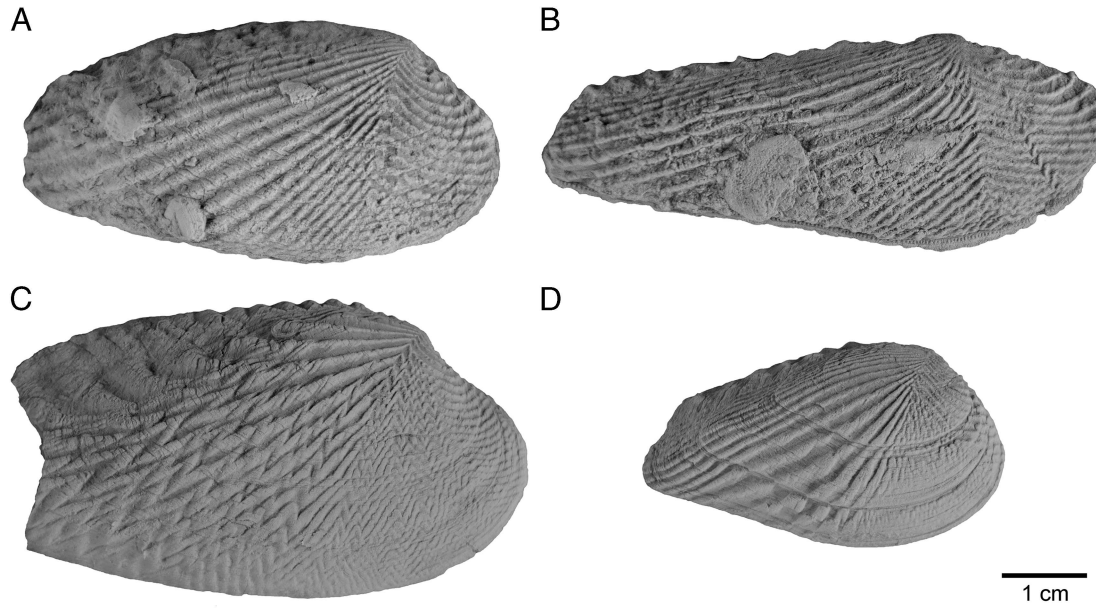

FIGURE 2. The four *Ptychomya* species addressed in this work. (A) *Ptychomya koeneni* (CPBA-23578.2), (B) *Ptychomya esbelta* (CPBA-23575.1), (C) *Ptychomya coihuicoensis* (CPBA-23601.1), and (D) *Ptychomya windhauseni* (CPBA-23597.3).

Materials and Methods

Materials.—All the studied material is housed in the Paleontological Collection of the University of Buenos Aires (CPBA) and comes from the Agua de la Mula, Bajada Vieja, Arroyo Truquicó, El Salado, Bajada del Agrio, Cerro Bayo, Arroyo Covunco, Gasoducto, Curaco Sur, and Pichaihue localities (Fig. 3). To guarantee a correct measurement of the size and shape of the shell, the material was carefully selected from a survey of several hundred (>1000) specimens, reducing the sample size to the 141 best-preserved ones. Each specimen was classified as belonging to *P. koeneni*, *P. esbelta*, *P. coihuicoensis*, or *P. windhauseni* based on their diagnostic characters (Milla Carmona et al. 2017) and photographed in left lateral view using a Canon PowerShot SX610 HS camera fixed on a tripod. The number of specimens of each species from each zone/subzone selected is shown in Table 1.

Temporal Framework.—We use the ammonoid-based biostratigraphic schemes developed by Aguirre-Urreta et al. (2007) and Aguirre-Urreta and Rawson (2012), who identify 10 ammonoid zones and 8 subzones for the Agrio Formation, dividing the column into a total of 15 consecutive biostratigraphic units, from which *Ptychomya* is recorded in 12. These zones/subzones can be correlated across the studied localities, providing a common temporal framework to work with (Fig. 4).

Recently, Aguirre-Urreta et al. (2015) provided U–Pb zircon radioisotopic ages for two tuff layers occurring at the base (base of the *S. riccardii* Zone, upper Hauterivian; ca. 129.09 Ma) and the top (top of the *P. groeberi* Zone, upper Hauterivian; ca. 127.42 Ma) of the Agua de la Mula Member (Fig. 4). To provide a temporal axis for subsequent time-series analyses, the thickness of each ammonoid zone/subzone is taken from data published by Lazo and Luci (2013) for Cerro Caicayén and Pichaihue; Guler et al. (2013) for Bajada Vieja; Aguirre-Urreta et al. (2008) for Agua de la Mula; Cataldo and Lazo (2016) for El Salado; and Aguirre-Urreta and Rawson (2012) for Mina San Eduardo. These sections correspond to expanded sedimentary successions, without significant hiatuses or interruptions in between, allowing estimation of the maximum thickness of each zone/subzone and thus intuitively reasonable estimations of maximum durations. The summed thicknesses of the zones from the Agua de la Mula Member and

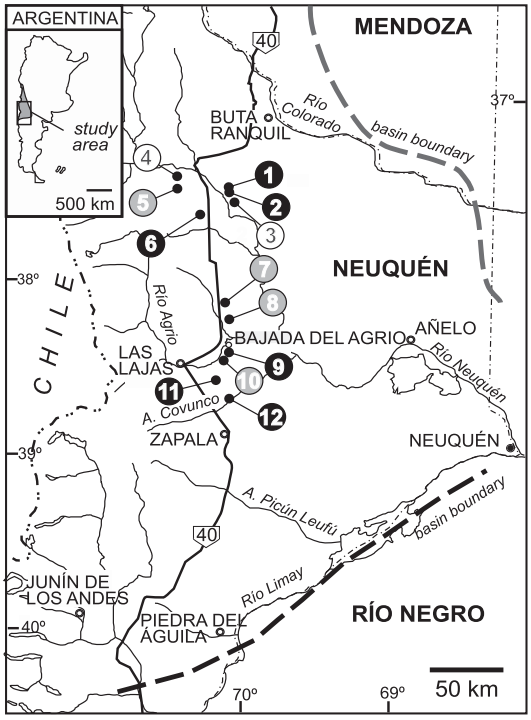

FIGURE 3. Map of the Neuquén Basin showing the localities sampled for specimens (black), successions (white), or both (gray). (1) Gasoducto (37°25′S, 69°26′W), (2) Curaco Sur (37°35′S, 70°00′W), (3) Mina San Eduardo (37°32′S, 70°00′W), (4) Cerro Caicayén (37°26′S, 70°24′W), (5) Arroyo Truquicó (37°28′S, 70°17′W), (6) Pichaihue (37°46′S, 70°13′W), (7) Agua de la Mula (38°03′S, 70°03′W), (8) El Salado (38°12′S, 70°03′W), (9) Bajada del Agrio (38°25′S, 70°00′W), (10) Bajada Vieja (38°25′S, 70°02′W), (11) Cerro Bayo (38°41′S, 70°04′W), and (12) Arroyo Covunco (38°42′S, 69°59′W). Modified from Milla Carmona et al. (2017).

the precise absolute ages from Aguirre-Urreta et al. (2015) are then used to estimate an average sedimentation rate, which in turn is used together with the maximum thicknesses of all the zones/subzones from Agrio Formation to calculate their maximum durations. We use these durations to calculate approximate average ages for each zone/subzone (Fig. 4). The continental Avilé Member is considered here as included in the time interval covered by the *W. vacaense* Zone, despite encompassing a hiatus at its base (which has been interpreted as a major sequence boundary; see Veiga et al. 2002). Although this implies an underestimation of the duration of the *W. vacaense* Zone and of the ages of zones/subzones from the Pilmatué Member, such bias is not expected to be severe or to affect the overall results from subsequent analyses.

TABLE 1. Number of specimens of each species per zone or subzone selected for morphometric and time-series analyses.

Zone/subzone	*P. koeneni*	*P. esbelta*	*P. coihuicoensis*	*P. windhauseni*
O. (O.) atherstoni	0	0	0	0
K. attenuatum	5	0	0	0
V. permolestus	0	0	0	0
P. angulatiformis	0	0	0	0
C. ornattum	0	1	0	0
D. crassicostatus	2	2	0	0
H. neuquensis	12	1	0	0
H. agrioensis	8	0	0	0
O. (O.) laticosta	1	2	0	0
H. gentilii	16	8	0	0
W. vacaense	6	1	0	0
S. riccardii	0	0	0	0
C. schlagintweiti	19	0	0	0
C. diamantensis	13	0	4	2
P. groeberi	0	0	1	21
S. riverorum	0	0	2	10

Morphometrics.—Two prominent external features of the shell, its outline and ribbing pattern, are quantified using geometric morphometric methods. The shell-outline shape of 137 specimens is quantified as a closed contour by means of a 2D elliptic Fourier analysis (Kuhl and Giardina 1982) using seven harmonics (Fig. 1C). Whenever the margin of the shell is chipped, the outline defined by an ontogenetically younger growth line of the same specimen is used instead. Ribbing pattern is a more complex trait to address. To produce a comparable measurement, the single posterior rib reaching the posterior ventral end of the shell and the anterior rib converging with it are selected as a reference and digitized as a series of 1000 (x, y) equally spaced coordinates (Fig. 1C). The shape of this reference pair of ribs is then quantified as an open contour through a 2D "extended coordinate analysis" (Milla Carmona et al. 2017): placement of three landmarks subdivides the curve (Fig. 1C) into two segments representing the commarginal anterior and subradial posterior ribs, each of which is standardized to an optimum (i.e., the lowest number of coordinates encompassing 99% of the perimeter of each segment for the most complex shape in the sample), constant number of (x, y) coordinates (105 and

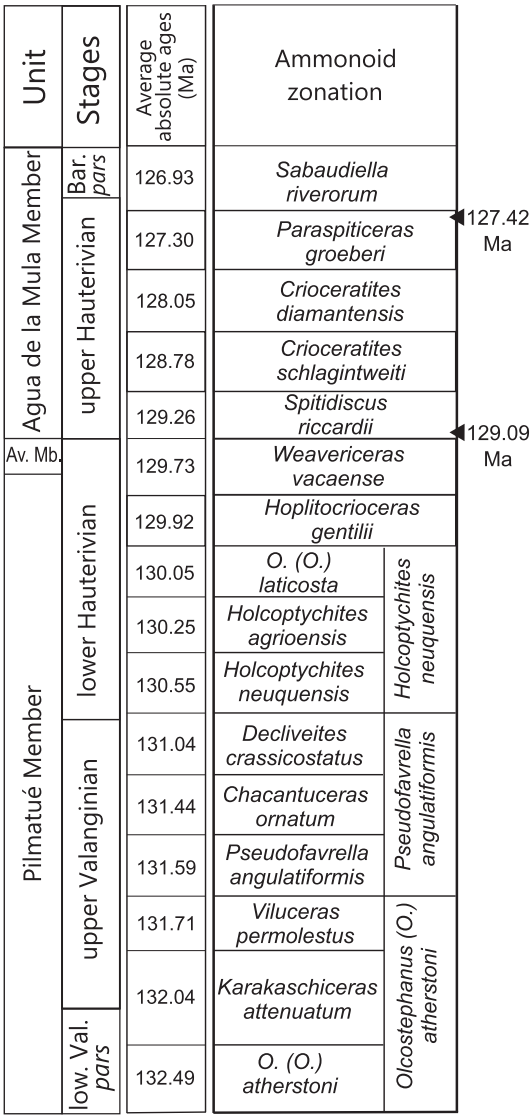

FIGURE 4. Temporal framework adopted for this study, showing the ammonoid zones or subzones used in this work (Aguirre-Urreta et al. 2007; Aguirre-Urreta and Rawson 2012), the relative position and inferred absolute age of the tuff layers dated by Aguirre-Urreta et al. (2015), and the approximate age calculated for each biostratigraphic unit. Abbreviations: Av. Mb., Avilé Member; Low. Val., lower Valanginian; Bar., Barremian.

300, respectively) following MacLeod (1999), and then aligned through Procrustes superimposition (Gower 1975; Rohlf and Slice 1990). These coordinates are not allowed to slide, because the sliding process severely distorts the intricate shape of the ribs of Ptychomya (see Supplementary Fig. 1), a problem that has been acknowledged and discussed elsewhere (MacLeod 2013). In both shell-outline and ribbing-pattern analyses, a principal component analysis is performed on the resulting shape descriptors (Fourier coefficients and superimposed coordinates, respectively). The first principal component resulting from the analysis of each trait is retained (from here onward, shell-outline and ribbing-pattern variables). Both shell-outline and ribbing-pattern variables are corrected for allometric variation by obtaining the residuals of a linear regression against size. For further details on the geometric morphometrics procedures undertaken, see Milla Carmona et al. (2017).

For shell size measurement, only gerontic specimens (Álvarez and Pérez 2016) are used. When a specimen reaches this ontogenetic stage, it slows down its growth along the sagittal plane (i.e., length and height) and accelerates its growth along the transverse axis (i.e., width). As a result, incremental growth lines (recognized using magnifying glasses) start to accumulate near the ventral margin, and the shell becomes more globose. Five landmarks are placed on the outlines of these specimens in lateral view, marking (1) the umbo, (2) the transition between dorsal and posterior margins, (3) the transition between posterior and ventral margins, (4) the point of maximum convexity of the ventral margin, and (5) the tip of the anterior margin (Fig. 1C). Unlike analysis of shell-outline shape, analysis of shell size requires using the full size of gerontic specimens. To do so, the position of landmarks in chipped sections of the margin is reconstructed using an iterative procedure, as follows. First, the position of the missing landmark(s) for a given specimen is estimated visually. Second, a reference configuration is constructed by placing the same five landmarks on the shell-outline averaged from the specimens of the same species and zone/subzone. Third, Procrustes superimposition is performed to align the landmark configurations of the specimen and the reference. Fourth, the visually estimated (x, y) positions are averaged with the (x, y) positions of the corresponding landmarks from the reference configuration. Fifth, the visually estimated (x, y) positions are replaced by the averaged (x, y)

ones. This procedure is repeated (using the averaged [x, y] coordinates instead of the visually estimated ones) until the Procrustes distance between the two configurations reduces to 1%. The ratio between the area of the initial and final polygons was used as a factor to correct the centroid size calculated from the initial configuration of landmarks, which in turn is used as the proxy for shell size.

The shell-outline, ribbing-pattern, and shell size variables are standardized (i.e., z-transformed to zero mean and unit variance) to facilitate comparison. All the morphometric procedures described are performed in the R environment (R Core Team 2016) using the 'R Base,' 'geomorph' (Version 3.0.1; Adams and Otárola-Castillo 2013), and 'Momocs' (Version 1.1.0; Bonhomme et al. 2014) packages, with the exception of the digitization of the coordinates for ribbing-pattern analysis, which is carried out using tpsDig (Version 2.26; Rohlf 2016).

Paleontological Time-Series Analysis.—Variation of morphology through time is assessed using the framework developed by Hunt (2006, 2008) for paleontological time-series analysis. In this approach, variation in mean morphology shown by a lineage through successive temporal levels is fit to different statistical models within a likelihood framework. Each statistical model constitutes the formalization of a classic, descriptive evolutionary pattern or model. The different models are compared by means of standard model-selection tools (typically, through the sample size–corrected Akaike information criterion [AICc] scores and derived Akaike weights), and the model that achieves the best balance between number of parameters and explanatory power is then selected as the preferred model of evolution. Paleontological time-series analyses are performed in the R environment using the package 'paleoTS' (Version 0.5.1; Hunt 2015).

We evaluate the fit of shell outline, ribbing pattern, and shell size of individual species and the genus as a whole to four basic models of evolution: general random walk (GRW), unbiased random walk (URW), stasis, and strict stasis. GRW and URW can be broadly described as directional and random evolution, respectively, whereas under stasis, morphology remains stable, showing no net evolutionary change. Strict stasis is a particular version of stasis in which morphology remains invariant through time. These simple models of evolution are not intended to be exact representations of the observed evolutionary modes. Rather, they constitute useful abstractions that allow the general characterization of the evolutionary dynamics shown by the studied lineages (Hunt 2007). Although more complex models are available, these four general models of evolution are an adequate choice for the analysis of sequences with a low number of temporal levels (Hunt et al. 2015), such as the present case (between 5 and 12 temporal levels). All models are fit using the joint parameterization (Hunt 2008).

Our data set presents two potentially serious problems regarding sample size, affecting inferences at different analytical levels. First, some combinations of species and zones/subzones (i.e., temporally restricted populations) present a very low number of specimens, some even at the extreme of being represented by a single individual (see Table 1). Low sample size at the population level casts doubts on the representativeness of the sample and can result in imprecise estimates of mean trait values. This is not so much a problem of lack of fossils as of preservation: the bulk of the sample was discarded for being laterally crushed, fragmented, or externally altered. We decided to include populations with a sample size of one or two specimens as long as they were reasonably representative of the morphology of the other conspecific, contemporaneous discarded specimens. Morphological variances for these "populations" are calculated by averaging the variance from specimen-rich populations from the same species lineage. The second problem is a low number of temporal steps. As paleontological time-series analysis use the mean trait value of successive levels from a stratigraphic sequence, the number of temporal steps in which a studied lineage is recorded effectively constitutes its sample size. For this reason, only lineages represented in at least five temporal steps were analyzed (G. Hunt personal communication 2017). Hence, the species restricted to the Agua de la Mula Member (*P. coihuicoensis* and

P. windhauseni), whose stratigraphic distributions span only three ammonoid zones, are not included in paleontological time-series analysis. Ribbing pattern and shell size of *P. esbelta* are not analyzed either, as these traits are measured in specimens from only four zones/subzones. However, since these species represent an important part of the evolutionary history of *Ptychomya* in the Agrio Formation in terms of stratigraphic representativeness, taxonomic diversity, and morphological variation, their patterns of change through time are still addressed descriptively in the "Results" section.

Disparity Analysis.—The shape disparity shown by the genus (not individual species) through time is addressed using variance as a proxy: variances of shell-outline and ribbing-pattern variables are calculated from pooled specimens from the Pilmatué and the Agua de la Mula Members. Significant differences in disparity are tested by constructing bootstrap (1000 permutations) 95% confidence intervals and assessing their degree of overlap. Disparity analysis is performed in the R environment.

Accompanying Biotic and Abiotic Factors.—To explore the possible association between biotic and abiotic factors and morphological evolution of *Ptychomya*, two additional sources of data are compiled: (1) the oxygen ($\delta^{18}O$) and carbon ($\delta^{13}C$) isotopic curves published by Aguirre-Urreta et al. (2008), and (2) the number of genera present in the associated bivalve fauna, taken from field observations and collection (CPBA) occurrences. Only genera interpreted as belonging to the same paleoecological guild of *Ptychomya* (i.e., shallow burrowers; Lazo 2007b) are counted. Data from the same zone/subzone are pooled together and averaged for integration into the same geochronologic scale used for the rest of the procedures undertaken. The resulting isotopic and paleodiversity curves are used as proxies for environmental stability and ecospace availability, respectively. These curves are then discussed and interpreted in the light of the published literature to explore potential processes driving the evolution of *Ptychomya*. Correlation between the two isotopic curves is examined by calculating the Pearson's correlation between the lagged differences (i.e., the vector of differences between values of consecutive zones/subzones) for the values of each isotope.

Results

The shell-outline variable constructed captures differences in the overall geometry of the shell corresponding to 89% of the total shell-outline shape variation. Higher scores represent elongated, subrectangular to suboval outlines with convex posterior ventral margins, whereas lower scores represent relatively shorter and higher shells with subtrapezoidal geometry and concave-downward posterior ventral margins (see shape-change vector from the vertical axis of Fig. 5A). The ribbing-pattern variable captures variation in the curvature and zigzagging of the reference pair of ribs, accounting for 71% of the total ribbing-pattern shape variation. Higher scores represent markedly concave-upward anterior and posterior ribs exhibiting marked zigzagging, whereas negative values represent slightly convex-upward posterior ribs and nearly straight, poorly developed anterior ribs (see shape-change vector from the vertical axis of Fig. 5B).

Results of paleontological time-series analyses are summarized in Tables 2 and 3. Change through time in mean trait values of the four species of *Ptychomya* and the genus as a whole is depicted in Figure 5. For the older pair of species (*P. koeneni* and *P. esbelta*), strict stasis is the best-supported model for all traits measured. Although shell outline and ribbing pattern of *P. koeneni* show no great support for this model (Akaike weight of the best-supported model is less than 2.7 times the weight of the next best-supported model; Hopkins and Lidgard 2012), the second best-supported model is stasis in both cases (Table 2). Ribbing pattern and shell size of *P. esbelta* seem to fluctuate around stable values, although the latter trait shows relatively wider fluctuations (Fig. 5B,C). *Ptychomya esbelta* shows a larger and more elongated shell than *P. koeneni* (Fig. 5A,C). Both species possess a very similar ribbing pattern, although *P. esbelta* shows slightly straighter to mildly concave-upward posterior ribs. On the other hand, although the younger pair of species (*P. coihuicoensis* and *P. windhauseni*) exhibit stable values for four of the six measured traits,

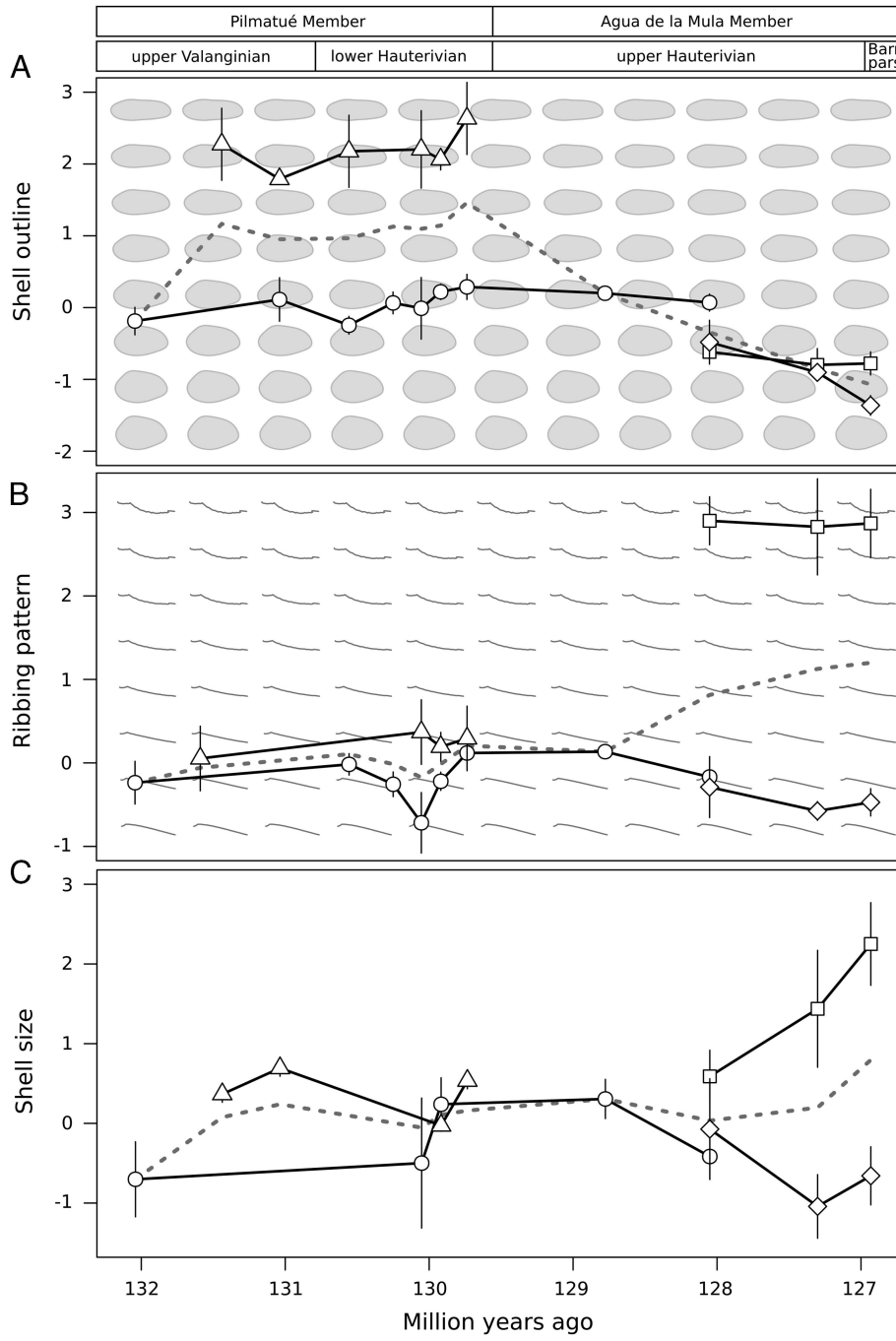

FIGURE 5. Morphological evolution of *Ptychomya*. (A) Mean shell-outline shape evolution. (B) Mean ribbing-pattern shape evolution. (C) Mean shell size evolution. Dashed line, *Ptychomya*; circles, *P. koeneni*; triangles, *P. esbelta*; squares, *P. coihuicoensis*; diamonds, *P. windhauseni*. The shapes in the background of plots A and B vary only in the vertical axis and were generated by sampling the shell-outline and ribbing-pattern variables at regular intervals and then premultiplying these scores by the inverse of the eigenvector matrix resulting from the PCA used to obtain each variable (see MacLeod 2009). These shapes, as well as the vertical axis scale of each plot, are expressed in the standard deviations of the corresponding variable. Bars are standard errors. Abbreviation: Barr., Barremian.

TABLE 2. Results from time-series analyses for traits measured at the species level. Bold indicates the best-supported evolutionary model for each case. Abbreviations: AICc, sample size–corrected Akaike information criterion score; GRW, general random walk; URW, unbiased random walk.

Species and trait	Model	Log likelihood	No. of parameters	AICc	Akaike weight
P. koeneni shell outline	GRW	−4.790	3	20.379	0.054
	URW	−6.181	2	18.362	0.148
	Stasis	−5.711	2	17.422	0.237
	Strict stasis	**−6.561**	**1**	**15.693**	**0.562**
P. koeneni ribbing patern	GRW	−7.553	3	27.106	0.009
	URW	−8.354	2	23.107	0.070
	Stasis	−6.762	2	19.924	0.343
	Strict stasis	**−8.109**	**1**	**18.886**	**0.577**
P. koeneni shell size	GRW	−4.083	3	38.167	0
	URW	−4.249	2	18.497	0.033
	Stasis	−4.021	2	18.041	0.041
	Strict stasis	**−4.249**	**1**	**11.831**	**0.926**
P. esbelta shell outline	GRW	−4.995	3	27.991	0.001
	URW	−5.139	2	18.278	0.070
	Stasis	−5.139	2	18.278	0.070
	Strict stasis	**−5.139**	**1**	**13.278**	**0.859**

TABLE 3. Results from time-series analyses for traits measured at the genus level. Bold indicates the best-supported evolutionary model for each case. Abbreviations: AICc, sample size–corrected Akaike information criterion score; GRW, general random walk; URW, unbiased random walk.

Species and trait	Model	Log Likelihood	No. of parameters	AICc	Akaike weight
Ptychomya shell outline	GRW	−11.329	3	31.659	0.183
	URW	**−11.668**	**2**	**28.670**	**0.816**
	Stasis	−19.080	2	43.493	0
	Strict stasis	−96.612	1	195.625	0
Ptychomya ribbing pattern	**GRW**	**−1.715**	**3**	**12.859**	**0.897**
	URW	−5.883	2	17.266	0.099
	Stasis	−9.155	2	23.810	0.004
	Strict stasis	−14.600	1	31.644	0
Ptychomya shell size	GRW	−4.568	3	19.136	0.061
	URW	−5.930	2	17.574	0.134
	Stasis	−5.930	2	17.574	0.134
	Strict stasis	**−5.930**	**1**	**14.359**	**0.670**

each species seem to present at least one variable evolving under a directional regime. Mean shell-outline shape of *P. windhauseni* shows a negative trend through time, attaining a very characteristic high, short, and posteroventrally projected shell-outline shape (Fig. 5A), while also being the smaller species of the cluster on average (Fig. 5C). Unlike this species' characteristic shell-outline shape and size, its ribbing pattern is almost identical to that of its putative ancestral species, *P. koeneni* (Fig. 5B). On the other hand, *P. coihuicoensis* shows an increasingly larger shell, quickly becoming the largest species of the cluster (Fig. 5C). Like *P. windhauseni*, *P. coihuicoensis* possesses relatively higher shells than its predecessors, although this trait remains stable at less extreme values during its evolutionary history (Fig. 5A). However, the trait that really distinguishes *P. coihuicoensis* (a ribbing pattern with relatively well-developed anterior ribs and markedly concave-upward, zigzagging posterior and anterior ribs) shows no sign of net change (Fig. 5B).

The average morphology inferred for the genus shows an increase in mean shell-outline score and shell size at the *C. ornatum* Subzone

(mid-upper Valanginian) related to the first occurrence of the larger and slenderer shell outline of *P. esbelta*. From that point until the top of the Pilmatué Member, at the *W. vacaense* Zone (uppermost lower Hauterivian), the mean shell-outline score and shell size of the genus remain stable. In the same interval, the mean ribbing-pattern score fluctuates but remains relatively constant around forms with poorly developed anterior ribs and straight posterior ribs with no zigzag arrangement. This pattern extends beyond the Pilmatué Member, until the *C. schlagintweiti* Zone (mid-upper Hauterivian). Therefore, the mean ribbing-pattern shape of the genus remains mostly unaffected by the appearance and subsequent extinction of *P. esbelta*.

During the upper Hauterivian–lowest Barremian interval, *Ptychomya* exhibits a different trend. At the base of the Agua de la Mula Member (lowermost upper Hauterivian) the mean shell-outline score of the genus drops, this time due to the extinction of *P. esbelta*. Shortly after, at the *C. diamantensis* Zone (mid-upper Hauterivian), the first occurrence of the relatively shorter and higher shells of *P. coihuicoensis* and *P. windhauseni* further decrease the mean shell-outline score of the genus. The extinction of the subrectangularly shaped *P. koeneni* (last occurring at the *C. diamantensis* Zone) and the directional anagenetic pattern of evolution displayed by *P. windhauseni* extend this trend until the last record of the genus in the Agrio Formation at the *S. riverorum* Zone (lowest Barremian). Simultaneously, the mean shell size of the genus remains stable at values similar to those observed at the top of the Pilmatué Member, showing only a slight final increment produced by the large shell size attained by *P. coihuicoensis* at the *S. riverorum* Zone. On the other hand, the mean ribbing-pattern score of the genus increases during the *C. diamatensis* and *P. groeberi* Zones due to the appearance of the highly disparate ribbing pattern of *P. coihuicoensis* and the extinction of *P. koeneni*.

The mean morphology of the genus in this geographic and stratigraphic setting is found to be evolving under a mix of evolutionary patterns (Table 3, Fig. 5). Whereas shell size exhibits strict stasis, shell-outline evolution is random: evolutionary change does occur, but shows no consistent direction. Ribbing pattern, on the other hand, shows a directional trend toward higher scores (i.e., more developed anterior ribs and concave-upward, zigzagging posterior ribs and) from the base to the top of the Agrio Formation. All three models are strongly supported (Table 3). Shell outline displays high disparity during the lower/upper Valanginian–lower Hauterivian interval, as expected given the disparate shell-outline shapes of *P. koeneni* and *P. esbelta*. However, it is significantly reduced in the upper Hauterivian–lowest Barremian, never recovering, despite the comparable number of species and the mixture of anagenetic patterns shown by *P. coihuicoensis* and *P. windhauseni* for this trait (Fig. 6A).

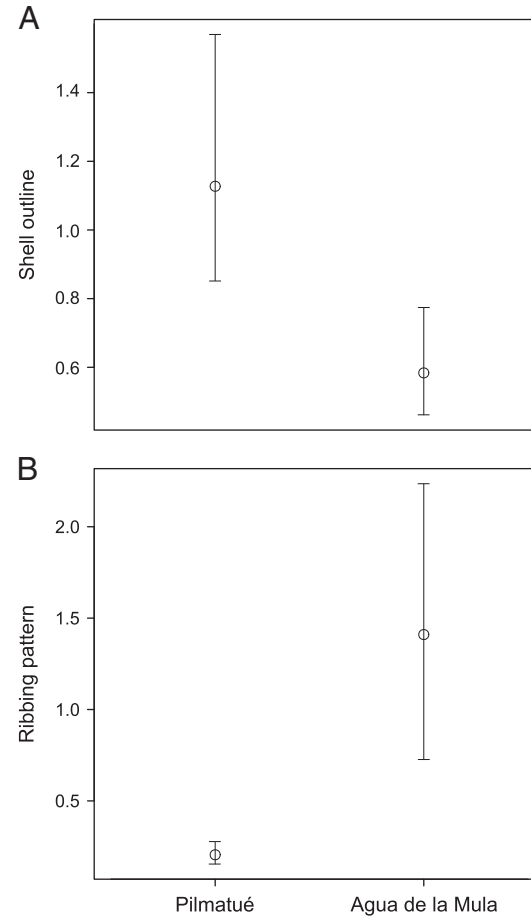

FIGURE 6. Comparison between morphological disparity shown by *Ptychomya* in the Pilmatué Member vs. the Agua de la Mula Member. (A) Shell-outline disparity. (B) Ribbing-pattern disparity. The vertical scale of each plot is expressed in the standard deviations of the corresponding variable. Bars represent 95% bootstrap confidence intervals for the disparity of each trait in each unit.

Ribbing-pattern disparity shows the opposite pattern: low values during the lower/upper Valanginian–lower Hauterivian and a marked increase for the upper Hauterivian–lowest Barremian, mainly due to the appearance of the highly disparate ribbing pattern of *P. coihuicoensis* (Fig. 6B).

Results of isotopic and paleoecological data compilation are shown in Figure 7. Both sources of data lack the *S. riverorum* Zone, as they were collected before the recognition of this zone from the top section of the *P. groeberi* Zone (and hence data from the former are pooled with data from the latter). Also, unlike morphological data, isotopic and shallow-burrowing bivalve records exist for the *O. (O.) atherstoni* Subzone and *S. riccardii* Zone from the Pilmatué and the Agua de la Mula Members, respectively. Both $\delta^{18}O$ and $\delta^{13}C$ show constantly fluctuating values throughout the studied interval (Fig. 7A). $\delta^{13}C$ shows its lowest values at the onset of the Pilmatué Member, during the *K. attenuatum* and *P. angulatiformis* Subzones (upper Valanginian), after which it remains relatively stable at higher values. $\delta^{18}O$ stays relatively stable at high values during the *K. attenuatum* Subzone–*H. gentilii* Zone before falling at the *W. vacaense*

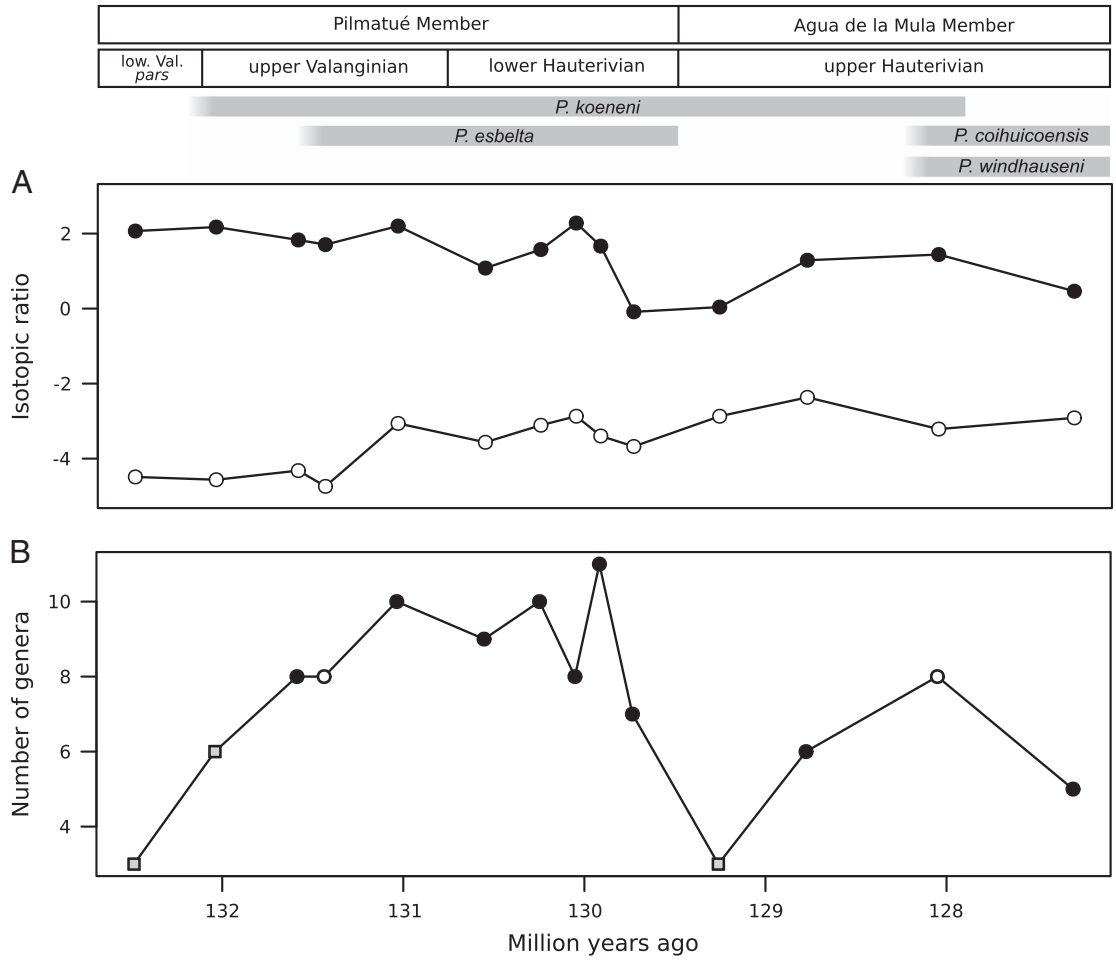

FIGURE 7. Isotopic and paleodiversity data compiled for the lower/upper Valanginian–uppermost Hauterivian interval. (A) Isotopic curves for carbon (filled circles) and oxygen (open circles). (B) Paleodiversity curve showing the number of shallow-burrowing bivalve genera present in the different zones or subzones; gray squares mark ammonoid zones for which dysoxic events have been recognized (see text), whereas open circles indicate first occurrences of *Ptychomya* species within this interval. Stratigraphic units and ranges of species are figured on top. Abbreviation: low. Val., lower Valanginian.

Zone. The curve rises again at the *C. schlagintweiti* Zone (upper Hauterivian), but never reaches the values attained during the Valanginian (Fig. 7A). Interestingly, during most of the interval covered by the Pilmatué Member, values of both isotopes increase and decrease together (Pearson's $r = 0.609$), although their fluctuations differ in magnitude. This correlation is not observed for the Agua de la Mula Member (Pearson's $r = 0.131$). Diversity of shallow-burrowing bivalves shows its lowest values at the onset of each member (*P. angulatiformis* Subzone, mid-upper Valanginian, and *S. riccardii* Zone, lower upper Hauterivian, respectively), with only three genera present. After these minima, the number of shallow-burrowing bivalve genera starts to rise in both units (Fig. 7B). In the Pilmatué Member, the number of genera stabilizes around 9, with a maximum of 11 genera occurring at the *H. gentilii* Zone (upper lower Hauterivian). For the Agua de la Mula Member, the overall generic diversity is lower, and the paleodiversity curve lacks the plateau attained in the Pilmatué Member. Instead, it reaches a maximum of 8 genera present at the *C. diamantensis* Zone (mid-upper Hauterivian), dropping immediately after (Fig. 7B).

Discussion

As noted by previous authors (e.g., Weaver 1931; Aguirre-Urreta et al. 2011), the morphological evolution of *Ptychomya* through the Lower Cretaceous of the Neuquén Basin is highly complex. Our results show that this complexity arises from the interaction between the characteristic morphologies and anagenetic patterns of evolution exhibited by the different species present, as well as the morphological change associated with speciation and extinction events within this interval. These factors, combined with the mosaic evolution of the addressed traits, result in changes in both the average morphology and the morphological disparity displayed by the genus at different moments of its evolutionary history.

Recent surveys on evolutionary modes in the fossil record found very low relative frequencies of directional evolution (5% to 10%) and high frequencies of stasis and random evolution, with a slight predominance of the latter (Hunt 2007; Hopkins and Lidgard 2012; Hunt et al. 2015). Our results do support a low incidence of directional evolution, as none of the traits analyzed at the species level is evolving under GRW (although the shell size of *P. coihuicoensis* and shell outline of *P. windhauseni* do show sustained accumulation of morphological change throughout their stratigraphic distribution). However, we also found a null incidence for URW in traits analyzed at the species level. Instead, our results show an overwhelming preponderance of stasis, with all traits analyzed at the species level showing no net morphological change. As mentioned earlier, qualitative assessment of the ribbing-pattern and shell size of *P. esbelta* and *P. windhauseni* and the ribbing pattern and shell outline of *P. coihuicoensis* shows overall stable values over time, concordant with a pattern of morphological stasis. Therefore, the evolution of *Ptychomya* in this particular geographic and stratigraphic setting represents a model in which stasis is predominant and change is mostly driven by the morphological shift associated with the emergence of new species. These two features represent the main predictions of the punctuated equilibria theory (Eldredge and Gould 1972; Gould and Eldredge 1977), and thus evolution of *Ptychomya* in the studied setting can be regarded as mostly speciational. The anagenetic accumulation of morphological change observed for some traits does not invalidate this evolutionary model, although it does complicate the evolutionary picture of this genus.

First occurrences of new species of *Ptychomya* in the Agrio Formation take place at two different times: the first at the *C. ornatum* Subzone (mid-upper Valanginian), when *P. esbelta* is initially recorded; and the second at the *C. diamantensis* Zone (mid-upper Hauterivian), when both *P. coihuicoensis* and *P. windhauseni* appear. As expected from a case of speciational evolution, transitional forms are not recorded; instead, species appear abruptly and show little or no net anagenetic evolution (with the exceptions of *P. coihuicoensis* shell size and *P. windhauseni* shell outline). The origin of any species can be considered to be at least as old as its first occurrence, but probably older. The extent of this delay is uncertain for our cluster of

species. However, assuming a punctuated model of evolution and considering the quality of the benthic invertebrate fossil record of the Agrio Formation, the average duration of a zone/subzone estimated for the studied interval (ca. 350 Kyr) and the estimated time required for marine invertebrates to complete cladogenesis (ca. 220 Kyr; Jackson and Cheetham 1999), it should encompass no more than one biostratigraphic level.

When contrasting timing of speciation with paleodiversity data, it becomes apparent that new *Ptychomya* species originate after times in which shallow-burrowing bivalve assemblages are depleted (*O. (O.) atherstoni–K. attenuatum* Subzones, *S. riccardii–C. schlagintweiti* Zones), appearing in the fossil record when this diversity is either recovering (*C. ornatum* Subzone) or reaching a peak (*C. diamantensis* Zone). The diversity minima coincide with the two most important transgressive episodes known in the Agrio Formation and the occurrence of two major events of marine dysoxia. These dysoxic events have been recognized at the bases of the Pilmatué and the Agua de la Mula Members by the presence of black shale deposits, high concentrations of total organic matter, low diversity, sometimes dwarfed invertebrate assemblages, and other paleoecological indicators of oxygen-controlled conditions (Tyson et al. 2005; Aguirre-Urreta et al. 2008; Guler et al. 2013; Cataldo and Lazo 2016). Guler et al. (2013) proposed that the enclosed geographic configuration the Neuquén Basin during the Early Cretaceous could have caused its temporary isolation from the Pacific Ocean, leading to reduced circulation, stratified water masses, and reduced seafloor oxygen levels, which in turn could have caused local extinction of benthic faunas. The diminished shallow-burrowing bivalve diversity would have resulted in greater ecological availability (Losos and Mahler 2010; Yoder et al. 2010). Therefore, the speciation events observed in *Ptychomya* during the Agrio Formation could have been triggered by ecological opportunity, a process widely accepted as a major driver of clade diversification and adaptive radiation (Wellborn and Langerhans 2015).

The anagenetic patterns of evolution shown here to characterize species of *Ptychomya* throughout the Agrio Formation fit surprisingly well to the model of plus ça change (Sheldon 1996). This model proposes that morphological stasis constitutes the usual response to geologically quickly fluctuating physical conditions, whereas directional evolution can be expected to occur in more gradually changing settings. Although both the Pilmatué and Agua de la Mula Members are inferred to have been deposited in highly cyclic, shallow-marine environments, they also present some important differences in terms of their overall environmental interpretation. In particular, the Pilmatué Member is characterized by a high cyclicity of lithofacies and aggradational succession of strata. Also, as mentioned earlier, carbon and oxygen curves, commonly used as proxies for organic matter input and temperature/salinity, respectively, show a rough correlation during the Pilmatué Member, increasing and decreasing together through the zones/subzones of this interval. The persistence of this relationship, despite fluctuations in their values, together with the stratigraphic arrangement of this unit, suggest the preponderance of some sort of fluctuating paleoenvironmental stability during the deposition of this unit. This situation changes for the interval covered by the Agua de la Mula Member, as the loss of correlation between isotopic values is accompanied by a general shallowing-upward trend, evidenced in the progradational (although still cyclic at a finer scale) succession of strata. Following the plus ça change model, the prevalence of stasis and lack of directional change observed for *P. koeneni* and *P. esbelta* in the Pilmatué Member would have been the result of the fluctuating (although stable at broader timescales) paleoenvironmental conditions inferred to predominate in the basin during the late Valanginian–early Hauterivian. On the other hand, the directional patterns of evolution shown by the younger *P. coihuicoensis* and *P. windhauseni* would reflect the evolutionary response of these species to the increasingly shallower conditions prevailing in the basin during the late Hauterivian–earliest Barremian.

Although alternative processes cannot be ruled out, the ecological opportunity and the plus ça change scenarios proposed here to explain different aspects of the evolution of *Ptychomya* seem particularly well suited to explain the observed evolutionary patterns in light of the complementary historical evidence. These hypotheses imply the adaptive nature of the morphological change displayed by the genus through the Agrio Formation, either associated with punctuations (i.e., rapid cladogenesis) or more slowly accumulated (i.e., anagenetic). However, although the traits addressed in this work are of undoubted adaptive significance for burrowing bivalves (Stanley 1970), a detailed morphofunctional model for these species has not been developed yet.

Conclusions

Throughout the Agrio Formation of the Neuquén Basin, the genus *Ptychomya* exhibits a complex pattern of morphological evolution. This complexity arises from three main sources of evolutionary variation, namely, (1) species turnover, (2) the mosaic evolution of different traits, and (3) the anagenetic pattern of evolution of each individual species lineage. Most of the addressed traits are found to be evolving under stasis, with two notable exceptions: shell outline of *P. windhauseni* and shell size of *P. coihuicoensis*, which show trends toward higher and larger shells, respectively. Therefore, the bulk of the evolutionary change displayed by the genus is associated with speciation events, aligning our results with the main predictions of the punctuated equilibria theory.

The timing of speciation and evolutionary patterns shown by the species lineages of *Ptychomya* can be explained by looking at the depositional history of the Agrio Formation. Origination of new species seems to be related to the ecological opportunity generated by two dysoxic episodes affecting the Neuquén Basin during the early/late Valanginian and earliest late Hauterivian, which are in turn associated with two local major transgressive episodes. After the first speciation event, in which *P. esbelta* appeared, and for the remainder of the late Valanginian–early Hauterivian, morphologies remained under stasis in response to the fluctuating, although to a broader scale stable, paleoenvironmental conditions. Partial desiccation and subsequent flooding of the basin triggered a second pulse of speciation, in which *P. coihuicoensis* and *P. windhauseni* appeared. The new, progressively shallower conditions somewhat changed the rules of the evolutionary game for *Ptychomya*, prompting the sustained accumulation of morphological change displayed by *P. coihuicoensis* and *P. windhauseni*.

Further research should be focused in two main directions: (1) the development of a thorough model of functional morphology for this genus and (2) the exploration of features of the evolution of other prominent bivalve genera from the Agrio Formation that are shared with *Ptychomya*. Both of these aspects need to be addressed to fully understand the details and extent of the adaptive processes driving the evolution of *Ptychomya* and to develop further insights into how the evolutionary processes operate at macroevolutionary scales.

Acknowledgments

We want to thank N. Mongiardino, O. Lehmann, D. Pérez, A. Elgorriaga, A. Toscano, C. Cataldo, and V. García Alonso for their helpful comments at different stages of this study. We are especially grateful to J. Crampton, G. Hunt, and one anonymous referee for useful comments and suggestions that greatly improved the article. This research was supported by grants ANPCyT PICT 2013-1506, UBACyT 20020130100106BA, CONICET PIP 11220120100542, and ANPCyT PICT 2015-1381 awarded to I. M. Soto, M. B. Aguirre-Urreta, V. A. Ramos, and D. G. Lazo, respectively. This is the contribution R-230 of IDEAN.

Literature Cited

Adams, D. C., and M. L. Collyer. 2009. A general framework for the analysis of phenotypic trajectories in evolutionary studies. Evolution 63:1143–1154.

Adams, D. C., and E. Otárola-Castillo. 2013. geomorph: an R package for the collection and analysis of geometric morphometric shape data. Methods in Ecology and Evolution 4:393–399.

Álvarez, J. M., and D. E. Pérez. 2016. Gerontic intraspecific variation in the Antarctic bivalve *Retrotapes antarcticus*. Ameghiniana 53:485–494.

Aguirre-Urreta, M. B., and P. F. Rawson. 2012. Lower Cretaceous ammonites from the Neuquen Basin, Argentina: a new heteromorph fauna from the uppermost Agrio Formation. Cretaceous Research 35:208–216.

Aguirre-Urreta, M. B., F. A. Mourgues, P. F. Rawson, L. G. Bulot, and E. Jaillard. 2007. The Lower Cretaceous Chañnarcillo and Neuquen Andean basins: ammonoid biostratigraphy and correlations. Geological Journal 42:143–173.

Aguirre-Urreta, M. B., G. D. Price, A. H. Ruffell, D. G. Lazo, R. M. Kalin, N. Ogle, and P. F. Rawson. 2008. Southern Hemisphere Early Cretaceous (Valanginian–early Barremian) carbon and oxygen isotope curves from the Neuquén Basin, Argentina. Cretaceous Research 29:87–99.

Aguirre-Urreta, M. B., D. G. Lazo, M. Griffin, V. Vennari, A. M. Parras, C. Cataldo, R. Garberoglio, and L. Luci. 2011. Megainvertebrados del Cretácico y su importancia bioestratigráfica. Relatorio del XVIII Congreso Geológico Argentino, 465–488.

Aguirre-Urreta, M. B., M. Lescano, M. D. Schmitz, M. Tunik, A. Concheyro, P. F. Rawson, and V. A. Ramos. 2015. Filling the gap: new precise Early Cretaceous radioisotopic ages from the Andes. Geological Magazine 152:557–564.

Archuby, F. M., M. Wilmsen, and H. A. Leanza. 2011. Integrated stratigraphy of the upper Hauterivian to lower Barremian Agua de la Mula Member of the Agrio Formation, Neuquen Basin, Argentina. Acta Geologica Polonica 61:1–26.

Blomberg, S. P., T. Garland, and A. R. Ives. 2003. Testing for phylogenetic signal in comparative data: behavioral traits are more labile. Evolution 57:717–745.

Bokma, F. 2002. Detection of punctuated equilibrium from molecular phylogenies. Journal of Evolutionary Biology 15:1048–1056.

Bonhomme, V., S. Picq, C. Gaucherel, and J. Claude. 2014. Momocs: outline analysis using R. Journal of Statistical Software 56:1–24.

Butler, M. A., and A. A. King. 2004. Phylogenetic comparative analysis: a modeling approach for adaptive evolution. American Naturalist 164:683–695.

Cataldo, C. S., and D. G. Lazo. 2016. Taxonomy and paleoecology of a new gastropod fauna from dysoxic outer ramp facies of the Lower Cretaceous Agrio Formation, Neuquén Basin, Argentina. Cretaceous Research 57:165–189.

Cheetham, A. H. 1986. Tempo of evolution in a Neogene bryozoan: rates of morphologic change within and across species boundaries. Paleobiology 12:190–202.

Eldredge, N., and S. J. Gould. 1972. Punctuated equilibria: an alternative to phyletic gradualism. Pp 83–115. *in* T. Schopf, ed. Models in paleobiology. Freeman, Cooper, San Francisco.

Gould, S. J. 2002. The structure of evolutionary theory. Harvard University Press, Cambridge.

Gould, S. J., and N. Eldredge. 1977. Punctuated equilibria: the tempo and mode of evolution reconsidered. Paleobiology 3:115–151.

Gower, J. C. 1975. Generalized Procrustes analysis. Psychometrika 40:33–51.

Guler, M. V., D. G. Lazo, P. J. Pazos, C. M. Borel, E. G. Ottone, R. V. Tyson, N. Cesaretti, and M. B. Aguirre-Urreta. 2013. Palynofacies analysis and palynology of the Agua de la Mula Member (Agrio Formation) in a sequence stratigraphy framework, Lower Cretaceous, Neuquén Basin, Argentina. Cretaceous Research 41:65–81.

Hannisdal, B. 2007. Inferring phenotypic evolution in the fossil record by Bayesian inversion. Paleobiology 33:98–115.

Harmon, L. J., J. A. Schulte, II, A. Larson, and J. B. Losos. 2003. Tempo and mode of evolutionary radiation in iguanian lizards. Science 301:961–963.

Harmon, L. J., J. B. Losos, J. Davies, R. G. Gillespie, J. L. Gittleman, W. B. Jennings, K. H. Kozak, M. A. McPeek, F. Moreno-Roark, T. J. Near, A. Purvis, R. E. Ricklefs, D. Schluter, J. A. Schulte, II, O. Seehausen, B. L. Sidlauskas, O. Torres-Carvajal, J. T. Weir, and A. Ø. Mooers. 2010. Early bursts of body size and shape evolution are rare in comparative data. Evolution 64:2385–2396.

Hopkins, M. J., and S. Lidgard. 2012. Evolutionary mode routinely varies among morphological traits within fossil species lineages. Proceedings of the National Academy of Sciences USA 109:20520–20525.

Howell, J. A., E. Schwarz, L. A. Spalletti, and G. D. Veiga. 2005. The Neuquén Basin: an overview. *In* G. D Veiga, L. A. Spalletti, J. A. Howell, and E. Schwarz, eds. The Neuquén Basin, Argentina: a case study in sequence stratigraphy and basin dynamics. Geological Society of London Special Publications. 252:1–14.

Hunt, G. 2006. Fitting and comparing models of phyletic evolution: random walks and beyond. Paleobiology 32:578–601.

——. 2007. The relative importance of directional change, random walks, and stasis in the evolution of fossil lineages. Proceedings of the National Academy of Sciences USA 104:18404–18408.

——. 2008. Evolutionary patterns within fossil lineages: model-based assessment of modes, rates, punctuations and process. *In* From evolution to geobiology: research questions driving paleontology at the start of a new century. Paleontological Society Papers 14:117–131.

——. 2015. paleoTS: analyze paleontological time-series. R package, Version 0.5-1. https://CRAN.R-project.org/package=paleoTS.

Hunt, G., M. A. Bell, and M. P. Travis. 2008. Evolution toward a new adaptive optimum: phenotypic evolution in a fossil stickleback lineage. Evolution 62:700–710.

Hunt, G., M. J. Hopkins, and S. Lidgard. 2015. Simple versus complex models of trait evolution and stasis as a response to environmental change. Proceedings of the National Academy of Sciences USA 112:4885–4890.

Jackson, J. B., and A. H. Cheetham. 1999. Tempo and mode of speciation in the sea. Trends in Ecology and Evolution 14:72–77.

Kucera, M., and B. A. Malmgren. 1998. Differences between evolution of mean form and evolution of new morphotypes: an example from Late Cretaceous planktonic foraminifera. Paleobiology 24:49–63.

Kuhl, F. P., and C. R. Giardina. 1982. Elliptic Fourier features of a closed contour. Computer Graphics and Image Processing 18:236–258.

Lazo, D. G. 2006. Análisis tafonómico e inferencia del grado de mezcla temporal y espacial de la macrofauna del Miembro Pilmatué de la Formación Agrio, Cretácico Inferior de cuenca Neuquina, Argentina. Ameghiniana 43:311–326.

——. 2007a. Análisis de biofacies y cambios relativos del nivel del mar en el Miembro Pilmatué de la Formación Agrio, Cretácico Inferior de la cuenca Neuquina, Argentina. Ameghiniana 44: 73–89.

——. 2007b. Early Cretaceous bivalves from the Neuquén Basin, west-central Argentina: notes on taxonomy, palaeobiogeography and palaeoecology. Geological Journal 42:127–142.

Lazo, D. G., and L. Luci. 2013. Revision of Valanginian Steinmanellinae bivalves from the Neuquén basin, west-central Argentina, and their biostratigraphic implications. Cretaceous Research 45:60–75.

Lazo, D. G., M. B. Aguirre-Urreta, G. D. Price, P. F. Rawson, A. H. Ruffell, and N. Ogle. 2008. Palaeosalinity variations in the Early Cretaceous of the Neuquén Basin, Argentina: evidence from oxygen isotopes and palaeoecological analysis. Palaeogeography, Palaeoclimatology, Palaeoecology 260:477–493.

Legarreta, L., and C. A. Gulisano. 1989. Análisis estratigráfico secuencial de la Cuenca Neuquina (Triásico Superior–Terciario Inferior, Argentina). *In* G. A. Chebli, and L. A. Spalletti, eds. Cuencas sedimentarias argentinas, Simposio de cuencas

sedimentarias argentinas. X Congreso Geológico Argentino, Tucuman. 221–243.

Losos, J. B., and D. L. Mahler. 2010. Adaptive radiation: the interaction of ecological opportunity, adaptation, and speciation. Pp 381–420. *in* M. A. Bell, D. J. Futuyma, W. F. Eanes, and J. S. Levinton, eds. Evolution since Darwin: the first 150 years. Sinauer, Sunderland, Mass.

MacLeod, N. 1999. Generalizing and extending the eigenshape method of shape visualization and analysis. Paleobiology 25:107–138.

——. 2009. Form and shape models. Palaeontological Association Newsletter 72:14–27.

——. 2013. Landmarks and semilandmarks: differences without meaning and meaning without difference. Palaeontological Association Newsletter 82:32–43.

Milla Carmona, P. S., D. G. Lazo, and I. M. Soto. 2016. Giving taxonomic significance to the morphological variability in the bivalve *Ptychomya* Agassiz. Palaeontology 59:139–154.

——. 2017. Taxonomy of the bivalve *Ptychomya* in the Lower Cretaceous of the Neuquén Basin (west-central Argentina). Papers in Palaeontology 3:219–240.

O'Meara, B. C., C. Ané, M. J. Sanderson, and P. C. Wainwright. 2006. Testing for different rates of continuous trait evolution using likelihood. Evolution 60:922–933.

Pagel, M., C. Venditti, and A. Meade. 2006. Large punctuational contribution of speciation to evolutionary divergence at the molecular level. Science 314:119–121.

Payne, L. P., J. R. Groves, A. B. Jost, T. Nguyen, S. E. Moffitt, M. H. Tessa, and J. M. Skotheim. 2012. Late Paleozoic fusulinoidean gigantism driven by atmospheric hyperoxia. Evolution 66: 2929–2939.

Pazos, P. J., D. G. Lazo, M. A. Tunik, C. A. Marsicano, D. E. Fernandez, and M. B. Aguirre-Urreta. 2012. Paleoenvironmetal framework of dinosaur tracksites and other ichnofossils in Early Cretaceous mixed siliciclastic-carbonate deposits in the Neuquen Basin, northern Patagonia (Argentina). Gondwana Research 22:1125–1140.

R Core Team 2016. R: a language and environment for statistical computing. R Foundation for Statistical Computing, Vienna, Austria. https://www.r-project.org.

Revell, L. J., M. A. Johnson, J. A. Schulte, II, J. J. Kolbe, and J. B. Losos. 2007. A phylogenetic test for adaptive convergence in rock-dwelling lizards. Evolution 61:2898–2912.

Rohlf, F. J. 2016. tpsDig, Version 2.26. Department of Ecology and Evolution, State University of New York at Stony Brook, Stony Brook, N.Y. http://life.bio.sunysb.edu/morph.

Rohlf., F. J., and D. E. Slice. 1990. Extensions of the Procrustes method for the optimal superimposition of landmarks. Systematic Zoology 39:40–59.

Sheldon, P. R. 1996. Plus ça change—a model for stasis and evolution in different environments. Palaeogeography, Palaeoclimatology, Palaeoecology 127:209–227.

Sidlauskas, B. 2008. Continuous and arrested morphological diversification in sister clades of characiform fishes: a phylomorphospace approach. Evolution 62:3135–3156.

Spalletti, L. A., D. G. Poiré, E. Schwarz, and G. D. Veiga. 2001. Sedimentologic and sequence stratigraphic model of a Neocomian marine carbonate–siliciclastic ramp: Neuquén Basin, Argentina. Journal of South American Earth Sciences 14:609–624.

Stanley, S. M. 1970. Relation of shell form to life habits of the Bivalvia (Mollusca). Geological Society of America Memoir 125:1–296.

Tyson, R. V., P. Esherwood, and K. A. Pattison. 2005. Organic facies variations in the Valanginian–mid-Hauterivian interval of the Agrio Formation (Chos Malal area, Neuquén Argentina): local significance and global context. *In* L. A. Spalletti, J. A. Howell, and E. Schwarz, eds. The Neuquén Basin, Argentina: a case of study in sequence stratigraphy and basin dynamics. Geological Society of London Special Publications. 252:251–266.

Veiga, G. D., L. S. Spalletti, and S. Flint. 2002. Aeolian/fluvial interactions and high resolution sequence stratigraphy of a non-marine lowstand wedge: the Avilé Member of the Agrio Formation (Lower Cretaceous), central Neuquén Basin, Argentina. Sedimentology 49:1001–1019.

Weaver, C. E. 1931. Paleontology of the Jurassic and Cretaceous of west-central Argentina. Memoirs of the University of Washington 1:1–595.

Wellborn, G. A., and R. B. Langerhans. 2015. Ecological opportunity and the adaptive diversification of lineages. Ecology and Evolution 5:176–195.

Yoder, J. B., E. Clancey, S. Des Roches, J. M. Eastman, L. Gentry, W. Godsoe, T. J. Hagey, D. Jochimsen, B. P. Oswald, J. Robertson, B. A. J. Sarver, J. J. Schenks, S. F. Spear, and L. J. Harmon. 2010. Ecological opportunity and the origin of adaptive radiations. Journal of Evolutionary Biology 23:1581–1596.